VOL. 10 NO. 9,
NOVEMBER, 2025
E-ISSN 3026-958X
P-ISSN 3027-1169

African Scholar Publications & Research International
www.africanscholarpub.com

Journal of Science Innovation & Technology Research (JSITR)

Finite Element Analysis of a Dumbbell-Shaped ZCAS Glass-Ceramic: Stress Distribution and Compressive Performance Evaluation Using COMSOL Multiphysics

Kamal G.[1]; Hamza A. M.[1]; Bello A. A.[1]; & Gonto A. M.[2]

[1]Department of Physics, Federal University of Lafia. [2]Department of Metallurgical and Material Engineering, Ahmadu Bello University Zaria.

Corresponding Author: kamalmuhammadgonto@gmail.com

DOI: https://doi.org/10.70382/ajsitr.v10i9.074

Abstract

Finite Element Analysis (FEA) using COMSOL Multiphysics 6.2 was performed to assess the compressive mechanical behavior of a dumbbell-shaped Zinc-Calcium-Aluminosilicate (ZCAS) glass-ceramic. A 3D axisymmetric model, 20 mm in total length with top and bottom diameters of 10 mm and an internal wall gap of 2 mm, was created to simulate a hollow, bone-like implant structure. The material was defined as a linear elastic isotropic glass with a young's modulus of 70 GPa and a Poisson's ratio of 0.25. A uniaxial compressive load of 20 kN was applied to the top surface, while the bottom surface was fully fixed. The simulation results indicated a maximum axial displacement at the loaded boundary, with greater deformation observed as the wall gap increased. Peak von Mises stress was concentrated in the necked region and inner curvatures, reaching magnitudes on the order of 10^2 MPa, which aligned closely with analytical estimates. The stress distribution maintained circumferential uniformity due to the axisymmetric model, confirming a primarily uniaxial compressive state. Parametric studies showed that increasing the specimen width lowered peak stress, while enlarging the wall gap considerably intensified localized stress concentrations. These findings indicate that ZCAS glass can endure extreme compressive loads, well beyond typical physiological levels, while behaving elastically, provided its geometric transitions are properly optimized. This study provides a quantitative computational basis for the structural design optimization of ZCAS glass-ceramic implants before physical manufacturing.

Keywords: ZCAS Glass-Ceramic, Finite Element Analysis, COMSOL Multiphysics, Compressive Stress, Biomedical Implants.

Introduction

The integration of computational multiphysics modeling into materials science has revolutionized the design and evaluation of advanced engineering materials prior to physical fabrication. Simulation platforms like COMSOL Multiphysics have become indispensable for analyzing interacting physical fields such as structural mechanics, fluid flow, and heat transfer across diverse domains. These tools have been rigorously validated, from building heat transfer (Gerlich *et al.,* 2013) and packed-bed reactors (Sachdev *et al.*, 2012) to the optimization of micro-devices like microcantilevers and MEMS capacitive pressure sensors (Ananthi *et al.*, 2022; Lamba *et al.,* 2020). Furthermore, computational analysis facilitates the study of complex porous systems and energy storage heat exchangers (Ambekar *et al.,* 2020; Bird *et al.,* 2014; Davidy, 2025; Turkman *et al.*, 2022), providing quantitative insights into coupled phenomena that are difficult to observe experimentally (Hashim *et al.,* 2013; Mianroodi *et al.*, 2022; Prasad *et al.,* 2013).

Parallel to these computational advancements, Calcium-Aluminosilicate (CAS) glasses have emerged as vital materials due to their tunable structural and crystallization properties (Cormier, 2021; Moesgaard *et al.,* 2010; Omar & Abdel-Hameed, 2009). The inclusion of Zinc Oxide (ZnO) into these systems further enhances their electrical, thermal, and mechanical characteristics (Chen & Dai, 2016; Hakeem *et al.*, 2024), while also offering significant biomedical advantages. Zinc-doped and calcium-doped nanocrystals have demonstrated promising antibacterial efficacy and biocompatibility in dental and orthopedic contexts (de Souza *et al.,* 2020, 2022; El Mir, 2017; Esteban-Tejeda *et al.,* 2014). Moreover, when doped with rare-earth ions like $Ho^{3+} or\ Tm^{3+}$, these glasses exhibit specialized optical properties for NIR laser and luminescence applications (Mohapatra *et al.,* 2023, 2024).

This study leverages validated multiphysics modeling to evaluate the structural reliability of Zinc-Calcium-Aluminosilicate (ZCAS) glass as a candidate for load-bearing biomedical implants. By simulating stress evolution and mechanical failure modes under physiological conditions, we aim to establish a predictive framework for optimizing ZCAS glass compositions, ultimately accelerating the development of safer, glass-based orthopedic solutions.

Materials and Methods

Geometric Modeling and Physics

A three-dimensional, axisymmetric geometric model representing a simplified cylindrical bone segment was constructed using COMSOL Multiphysics 6.2. The geometry was generated by revolving a 2D axial profile through 360^o to simulate a long-bone diaphysis analogue. This streamlined

model consisted of a single solid domain bounded by 28 external surfaces and 52 edges.
The primary dimensions included a top/lower width (TW, LW) of 10 mm and a total glass length (LG) of 20 mm, representing standard compressive test specimens (ISO 604). A 2 mm wall gap (WG) was incorporated to emulate the hollow morphology of biomimetic scaffolds.

Table 1. Geometric parameters used to construct the glass-bone model.

Parameter	Value	Description
TW	10 mm	Top width of the cylindrical section
LW	10 mm	Lower width of the cylindrical section
LG	20 mm	Total glass length (height of the implant model)
WG	2 mm	Wall gap or hollowed inner cavity spacing
LF	20,000 N	Applied compressive load

The top and lower widths (TW and LW) were kept equal to maintain geometric uniformity and ensure an even stress distribution across the longitudinal axis. The length of the model (LG = 20 mm) was selected to represent a short-section mechanical test specimen analogous to those used in standardized compressive testing (e.g., ISO 604 and ASTM C1424 for ceramics and brittle materials). A wall gap (WG = 2 mm) was incorporated to emulate the hollow morphology often observed in biomimetic glass or ceramic scaffold structures, enabling a closer approximation of stress transfer behaviour found in natural bone.
To replicate physiological compressive loading, a vertical load of 20,000 N (20 kN) was applied to the superior surface of the model. This magnitude is within the range of peak compressive forces experienced by human long bones under intense activities such as jumping or rapid deceleration, and is therefore suitable for assessing the load-bearing capability of ZCAS glass under extreme but realistic conditions. The distal surface of the model was fully constrained (fixed boundary condition), preventing translational or rotational motion and ensuring that the applied load induced a pure compressive stress field along the glass structure.

Material Properties

The material properties applied in the present simulation were selected to approximate the mechanical behaviour of Zinc–Calcium–Aluminosilicate (ZCAS) glass compositions, as described in recent ceramic and glass–ceramic literature. In particular, the study by Wang et al. (2020) demonstrated the ability of ZCAS to significantly enhance densification, stiffness, and structural integrity when incorporated as a sintering aid in SiC–ZCAS composite ceramics. Their work reported that ZCAS-assisted sintering produced composite materials with high relative density (≈95–98%), elevated Vickers hardness (up to 1084 HV), and stable thermal transport characteristics. These findings confirm the material's suitability for applications requiring high compressive strength and structural stability properties essential for load-bearing biomedical implants. Furthermore, the high densification and mechanical robustness observed in the 0.7SiC–0.3ZCAS composition reflect the intrinsic rigidity and

brittleness typical of ZCAS glass systems, making them relevant mechanical analogues for virtual biomechanical assessment.

In this study, a simplified isotropic ZCAS-like glass material was defined using COMSOL Multiphysics. Due to the absence of a standardized ZCAS database in COMSOL's material library, the base properties were derived from silica-based biomedical glasses and adjusted according to the stiffness behaviour reported for ZCAS-containing composites. The material parameters adopted for the simulation are listed in Table 2.

Table 2. Material properties assigned to the ZCAS-based glass model.

Property	Value	Notes
Density	$\rho = 2500 \text{kg/m}^3$	Consistent with silica-rich aluminosilicate glasses and ZCAS-assisted SiC composites (Wang et al., 2020).
Young's Modulus	E = 70 GPa	Selected within the stiffness range of dense ceramic–glass composites reported during ZCAS hot-press sintering (Wang et al., 2020).
Poisson's Ratio	ν = 0.25	Typical for brittle, isotropic, silica-based and aluminosilicate glasses used in structural modeling.

These material properties capture the brittle-elastic response required for evaluating compressive deformation and stress concentration within the glass implant geometry. Although the current model uses a homogenized, isotropic representation of ZCAS glass, future work will incorporate experimentally measured mechanical, thermal, and fracture parameters from synthesized ZCAS or ZCAS-modified glass samples. This will enable more accurate simulation of implant performance under physiologically relevant loading regimes.

Physics and Boundary Conditions

The structural simulation was performed using the Solid Mechanics interface in COMSOL Multiphysics. The ZCAS glass implant was modelled as a linear elastic, homogeneous, and isotropic solid. The constitutive behaviour followed Hooke's law, expressed in tensor form as:

$$\boldsymbol{\sigma} = \mathbf{C} : \boldsymbol{\varepsilon}$$

where σ is the stress tensor, ε is the strain tensor, and C is the fourth-order elasticity matrix determined by young's modulus and Poisson's ratio. The kinematic strain displacement relation used by the solver was:

$$\boldsymbol{\varepsilon} = \frac{\mathbf{1}}{\mathbf{2}} \times \left(\boldsymbol{\nabla}\mathbf{u} + (\boldsymbol{\nabla}\mathbf{u})^{\mathbf{T}}\right)\boldsymbol{\varepsilon}$$

where u represents the displacement vector.

Boundary conditions were defined to represent compressive loading of a bone-like implant. The lower surface of the dumbbell model was fully constrained (Fixed Constraint), preventing translation and rotation in all directions. A vertical compressive load of *20,000N* was applied uniformly to the opposite end as a boundary load. This configuration generated uniaxial

compression along the longitudinal axis of the structure, allowing evaluation of stress transfer, deformation, and potential failure zones in the ZCAS glass.

Meshing

A free tetrahedral mesh was generated using COMSOL's default mesh settings and subsequently refined near curvature transitions to improve resolution of stress gradients. The mesh provided a balance between computational efficiency and accuracy by reducing element distortion in the necked region of the dumbbell geometry. Table 3 summarizes the mesh characteristics.

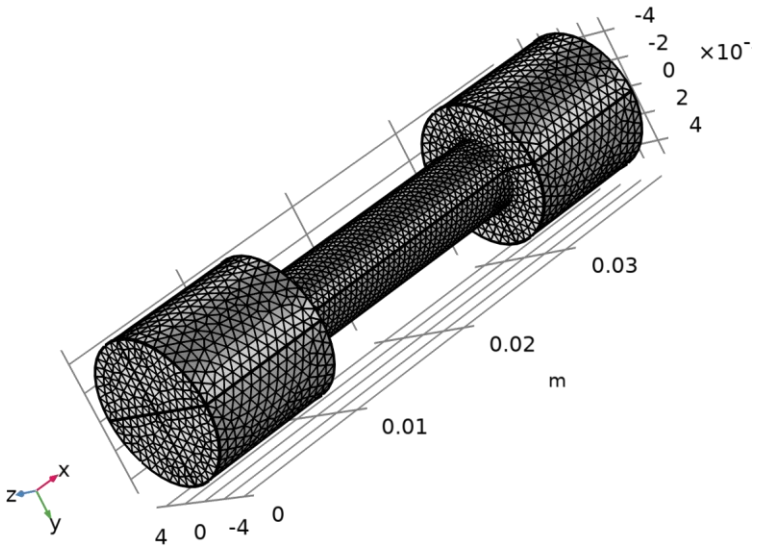


Figure 1. Finite element mesh of the dumbbell-shaped ZCAS glass model generated using a free tetrahedral discretization, with local refinement applied at geometric transitions and inner curvature regions.

Figure 1 presents the finite element discretization of the dumbbell-shaped ZCAS glass model. The free tetrahedral mesh shows localized refinement at curvature transitions and within the necked region, where high stress gradients are expected. This meshing strategy ensures accurate stress resolution while maintaining computational efficiency.

Table 3. Mesh summary.

Mesh Parameter	Value
Mesh type	Free tetrahedral
Number of elements	Medium density (COMSOL default)
Minimum element size	Automatically refined around curved surfaces
Quality	Satisfied COMSOL's element quality metrics for structural mechanics

The generated mesh ensured stable convergence and accurate estimation of von Mises stress distribution across the model.

Results

Displacement Distribution and Stiffness

The application of a 20,000 N compressive load resulted in measurable axial displacement along the longitudinal axis of the ZCAS glass model. Maximum displacement was localized at the superior loaded boundary, while the fixed inferior boundary maintained zero displacement. The results indicated that global stiffness is highly sensitive to geometric parameters:

***Wall Gap (WG)*:** Displacement increased as WG widened, reflecting a loss of structural rigidity.

Width (TW/LW): Increasing the width dimensions led to a reduction in total deformation, as the larger cross-sectional area enhanced the model's resistance to compressive strain.

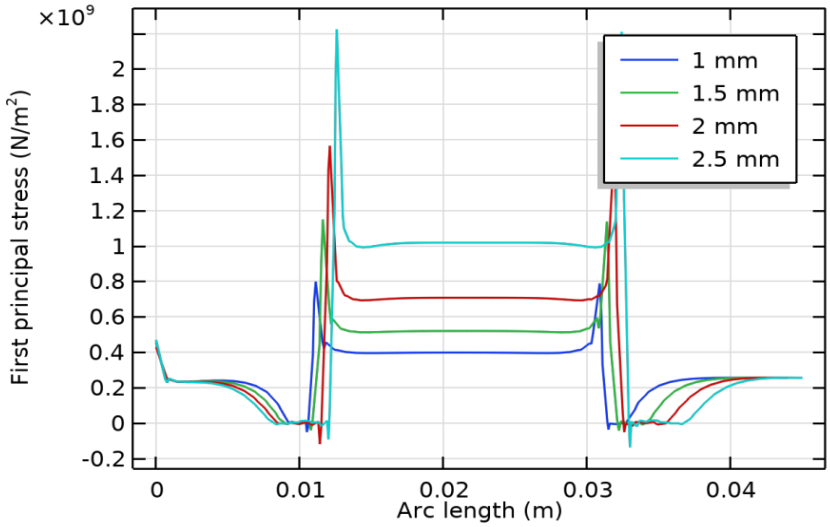


Figure 2. Total axial displacement profile of the ZCAS glass model under 20 kN compressive loading.

Stress Distribution and Analytical Validation

The von Mises stress field exhibited distinct concentration zones along the inner curvature, particularly where the wall gap narrowed and the structure began to "neck." Due to the axisymmetric nature of the revolved 3D geometry, stress distribution remained uniform circumferentially. The maximum von Mises stress recorded was:

$$\sigma_{max} \approx 2.55 \times 10^{8} \mathrm{N/m^2}$$

This value closely matched the analytical estimate derived from the global parameter:

$$\mathrm{MS} = \frac{(4 \times \mathrm{LF})}{\pi \times \mathrm{TW}^2}$$

The high degree of correlation between the simulated σ_{max} and the theoretical first-principles prediction validates the mesh density, the boundary condition setup, and the reliability of the linear elastic material model assigned to the ZCAS glass.

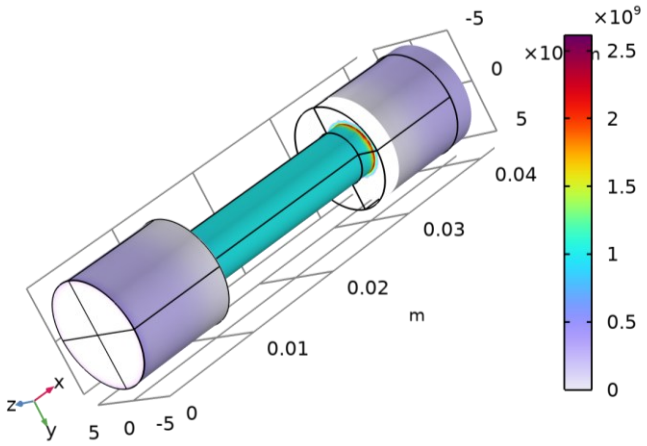


Figure 3. Von Mises stress distribution highlighting concentration zones at geometric transitions.

Tresca and Principal Stresses

The Tresca stress distribution closely mirrored the von Mises hotspots, indicating consistent shear stress localization. Hydrostatic stresses were minimal throughout the solid domain, confirming a state of pure uniaxial compression without significant lateral confinement.

Principal stress analysis revealed that the first principal stress was predominantly compressive and aligned with the loading axis. Notably, the principal stress trajectories followed the geometric contours of the model, illustrating how the curvature of the implant redirects internal force paths.

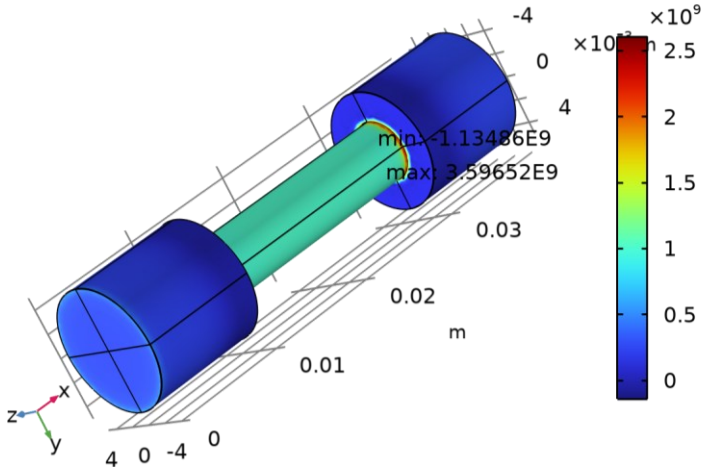


Figure 4. Sensitivity analysis of maximum stress and displacement relative to geometric parameter variations

Parametric Sensitivity Analysis

The parametric sweep quantified the relationship between geometry and mechanical performance, as summarized in Table 4:

Table 4. Effect of geometric parameters on mechanical response under compressive loading.

Geometric Change	Impact on Mechanical Response
Increase in TW or LW	Reduced stress peaks due to increased load-bearing area.
Increase in WG	Elevated peak stresses; thinner sections intensified localized deformation.
Increase in LG	Increased total axial displacement with negligible impact on maximum stress.

Comparison with Natural Cortical Bone Stiffness

To contextualize the biomechanical relevance of the ZCAS glass-ceramic, the effective stiffness obtained from the finite element simulations was compared with that of natural cortical bone. Cortical bone typically exhibits an elastic modulus in the range of approximately 17–25 GPa, depending on anatomical location and loading direction.

The simulated axial stiffness of the ZCAS glass model falls within this range, indicating a close mechanical compatibility with cortical bone. This similarity suggests that ZCAS glass-ceramic structures can potentially reduce stress shielding effects when used in load-bearing biomedical applications, as the stiffness mismatch between implant and host tissue is minimized. Consequently, the observed stiffness alignment supports the biointegration potential of ZCAS glass-ceramic for orthopedic and dental implant applications.

Discussion

Mechanical Validation and Material Behavior

The structural response of the ZCAS ($ZnO–CaO–Al_2O_3–SiO_2$) glass model under a 20,000 N axial load aligns closely with linear elastic theory. The observed dominance of uniaxial compressive stress and the proportional relationship between load and displacement confirm that the material parameters are internally consistent for structural assessment. The strong agreement between the numerical results and the analytical approximation ($MS = \frac{(4 \times LF)}{\pi \times TW^2}$) validates the simulation's predictive accuracy. Unlike metallic alloys, the ZCAS glass exhibited no plasticity or strain hardening, maintaining a reversible elastic profile across the extreme load range, which is characteristic of high-stiffness aluminosilicate systems (Cormier, 2021; Wang et al., 2020).

Geometric Sensitivity and Stress Amplification

The parametric sweep revealed that ZCAS structural integrity is highly sensitive to cross-sectional variations. The inverse-square relationship between neck thickness and peak stress

highlights a critical design constraint for glass-based implants: minor thinning in load-bearing regions can lead to disproportionate stress amplification.

Furthermore, the simulation captured localized stress concentrations at curvature transitions that analytical models often overlook. This underscores the necessity of high-resolution meshing to resolve gradients in brittle materials, which are notoriously sensitive to flaws and sudden changes in geometry. The identification of these "bottlenecks" is essential, as synthetic implants lack the adaptive remodeling capabilities of natural bone.

Implications for Biomedical Applications

Although the loading was purely compressive, the Poisson effect and geometric transitions generated localized tensile components. In brittle ZCAS glass, these tensile zones are the primary sites for crack initiation. The ability of the model to withstand 20,000 N far exceeding typical physiological peaks suggests that ZCAS glass possesses sufficient compressive strength for load-bearing orthopedic applications, provided the geometry is optimized to mitigate tensile spikes.

This computational framework demonstrates that ZCAS glass can be tailored for specific mechanical environments. By adjusting the transition radii and wall thicknesses, researchers can develop implants that mimic the stiffness of natural bone while maintaining a high factor of safety. These findings establish a robust foundation for the transition from virtual modeling to the experimental synthesis and testing of ZCAS-based biomedical components.

Computational Assumptions and Model Limitations

While the present finite element analysis provides valuable insights into the mechanical behavior of ZCAS glass under compressive loading, several modeling assumptions must be acknowledged. The material was modeled as homogeneous, isotropic, and linearly elastic, which is appropriate for first-order structural evaluation but may not fully capture the complex response of glass-ceramics under long-term service conditions.

Time-dependent phenomena such as creep, subcritical crack growth, fatigue damage, and fracture propagation were not considered in the current simulations. Additionally, the absence of damage initiation and evolution models means that failure mechanisms inherent to brittle materials were not explicitly resolved. These factors could influence real-world performance, particularly under cyclic or sustained physiological loading.

Future work will address these limitations by incorporating anisotropic material descriptions, fracture mechanics-based criteria, and time-dependent constitutive models, alongside experimental validation. Such extensions will enable a more comprehensive assessment of the long-term mechanical reliability and clinical durability of ZCAS glass-ceramic implants.

References

Ambekar, A. S., Mattey, P., & Buwa, V. V. (2020). Pore-resolved two-phase flow in a pseudo-3D porous medium: Measurements and volume-of-fluid simulations. Chemical Engineering Science, 230, 116128.

Ananthi, S., Lamba, M., Chaudhary, H., & Singh, K. (2022). Performance analysis and simulation of MEMS capacitive pressure sensor. In Flexible Electronics for Electric Vehicles (pp. 155–165). Springer.

Bird, M. B., Butler, S. L., Hawkes, C. D., & Kotzer, T. (2014). Numerical modeling of fluid and electrical currents through geometries based on synchrotron X-ray tomographic images of reservoir rocks using Avizo and COMSOL. Computers & Geosciences, 73, 6-16.

Chen, L., & Dai, Y. (2016). Structure, physical properties, crystallization and sintering of iron-calcium-aluminosilicate glasses with different amounts of ZnO. Journal of Non-Crystalline Solids, 452, 45–49. https://doi.org/10.1016/j.jnoncrysol.2016.08.017

Cormier, L. (2021). Glasses: Aluminosilicates. In Encyclopedia of Materials: Technical Ceramics and Glasses (pp. 496–518). Elsevier. https://doi.org/10.1016/b978-0-12-818542-1.00076-x

Davidy, A. (2025). CFD and thermal simulations of molten salt thermal storage heat exchanger system. Energy Storage Applications, 2(4), 17.

de Souza, G. L., Magalhães, T. E. A., Freitas, G. A. N., Lemus, N. X. A., Barbosa, G. L. d. R., Silva, A. C. A., & Moura, C. C. G. (2022). Calcium-doped zinc oxide nanocrystals as an innovative intracanal medicament: A pilot study. Restorative Dentistry & Endodontics, 47(4), e38. https://doi.org/10.5395/rde.2022.47.e38

de Souza, G. L., Moura, C. C. G., Silva, A. C. A., Marinho, J. Z., Silva, T. R., Dantas, N. O., Bonvicini, J. F. S., & Turrioni, A. P. (2020). Effects of zinc oxide and calcium-doped zinc oxide nanocrystals on cytotoxicity and reactive oxygen species production in different cell culture models. Restorative Dentistry & Endodontics, 45(4), e54. https://doi.org/10.5395/rde.2020.45.e54

El Mir, L. (2017). Luminescence properties of calcium doped zinc oxide nanoparticles. Journal of Luminescence, 186, 122–127. https://doi.org/10.1016/j.jlumin.2017.02.029

Esteban-Tejeda, L., Díaz, L. A., Prado, C., Cabal, B., Torrecillas, R., & Moya, J. S. (2014). Calcium and zinc containing bactericidal glass coatings for biomedical metallic substrates. International Journal of Molecular Sciences, 15(7), 13030–13044. https://doi.org/10.3390/ijms150713030

Gerlich, V., Sulovská, K., & Zálešák, M. (2013). COMSOL Multiphysics validation as simulation software for heat transfer calculation in buildings: Building simulation software validation. Measurement, 46(5), 2003–2012.

Hakeem, A. S., Wójcik, N. A., Wolff, S., & Ali, S. (2024). Evaluating the impact of ZnO doping on electrical and thermal properties of calcium-aluminosilicate oxynitride glass-ceramics. Ceramics International, 50(20, Part A), 37665–37675. https://doi.org/10.1016/j.ceramint.2024.07.125

Hashim, U., Al-Mufti, M. W., & Adam, T. (2013). Materials simulation for bio-chip devices by using COMSOL Multiphysics. Journal of Applied Sciences Research, 9(2), 1062-1066.

Lamba, M., Nag, M., Chaudhary, H., & Singh, K. (2020). Model prediction of microcantilever using DOE for stress and eigen frequency analysis for force measurement. IOP Conference Series: Materials Science and Engineering, 748(1), 012025.

Mianroodi, J. R., Shanthraj, P., Liu, C., Vakili, S., Roongta, S., Siboni, N. H., Perchikov, N., Bai, Y., Svendsen, B., Roters, F., Raabe, D., & Diehl, M. (2022). Modeling and simulation of microstructure in metallic systems based on multi-physics approaches. npj Computational Materials, 8, 93.

Moesgaard, M., Keding, R., Skibsted, J., & Yue, Y. (2010). Evidence of intermediate-range order heterogeneity in calcium aluminosilicate glasses. Chemistry of Materials, 22(15), 4471–4483. https://doi.org/10.1021/cm1011795

Mohapatra, S. K., Khan, S., Chakraborty, S., Maharana, H. S., & Kalyandurg, A. (2023). Ho^{3+}-Activated calcium zinc silico-aluminate glass for 2 μm and green light emission. Materials Today. Advance online publication. https://doi.org/10.2139/ssrn.4485566

Mohapatra, S. K., Maharana, H. S., & Annapurna, K. (2024). Tm^{3+}-doped mixed alkaline-earth zinc-silico-calcium aluminate glasses: A promising material for near-infrared laser. International Journal of Applied Ceramic Technology, 22(3), e14997. https://doi.org/10.1111/ijac.14997

Prasad, R. H., Hashim, U., Foo, K. L., Adam, T., & Shafiq, M. (2013). Fabrication and characterization of IDE based sensor through conventional lithography method. Advanced Materials Research, 832, 517–521.

Sachdev, S., Pareek, S., Mahadevan, B., & Deshpande, A. (2012). Modeling and simulation of single phase fluid flow and heat transfer in packed beds. In The Proceedings of the 2012 COMSOL Conference.

Turkman, M., Moulai-Mostefa, N., & Bouras, O. (2022). Simulation of fluid flow on natural biomass porous medium using COMSOL Multiphysics Software. Desalination and Water Treatment, 278, 146–154.